

Abd El-Aziz S. Fouda<sup>1\*</sup>, Ibrahim S. El-Hallag<sup>2</sup>,  
Ahmed A. El-Barbary<sup>2</sup>, Fatma M. El Salamony<sup>1</sup>

<sup>1</sup>Department of Chemistry, Faculty of Science, Mansoura University,  
Mansoura-35516, Egypt, <sup>2</sup>Department of Chemistry, Faculty of Science,  
Tanta University, Tanta, Egypt

Scientific paper

ISSN 0351-9465, E-ISSN 2466-2585

<https://doi.org/10.62638/ZasMat1150>



Zastita Materijala 65 (2)  
331 - 342 (2024)

## Electrochemical and theoretical evaluations of 3-(4-chlorophenyl)-7-methyl-5H-[1, 2, 4] triazolo [3,4-b][1,3,4]thiadiazin-6(7H)-one as corrosion inhibitor for copper in nitric acid environment

### ABSTRACT

3-(4-chlorophenyl)-7-methyl-5H-[1,2,4]triazolo[3,4-b][1,3,4]thiadiazin-6(7H)-one (CTT) was synthesized and evaluated as corrosion inhibitor for copper in one molar  $\text{HNO}_3$ . The adsorption properties for the synthesized CTT were determined by experimental and theoretical methods in acid environment. The chemical method such as mass loss method (ML), DC potentiodynamic polarization (PDP) and AC impedance (EIS) techniques were utilized to determine the inhibitive behavior of CTT. Outcome data obtained from these methods displayed that with increasing the concentration of CTT its inhibition efficiencies (%IE) increases and reached 91.5% at  $24 \times 10^{-6} \text{ M}$ ,  $25^\circ\text{C}$  using EIS technique. The presence of CTT reduces the capacity of the double layer ( $C_{dl}$ ) and improves the charge transfer resistance ( $R_{ct}$ ) in a solution of one molar nitric acid. CTT is a mixed-type inhibitor from the data obtained from the polarization curves. The attained data indicated that CTT was physically adsorbed onto the Cu surface in accordance for the Langmuir adsorption. The surface protection examination was carried out using scanning electron microscopy (SEM), Energy Dispersive X-ray (EDX) and atomic force microscope (AFM). Also, The quantum chemical parameters of CTT were computed and discussed. The results of several methods are in agreement with each other.

**Keywords:** Corrosion inhibition, Copper, Nitric acid, 3-(4-chlorophenyl)-7-methyl-5H-[1,2,4]triazolo[3,4-b][1,3,4]thiadiazin-6(7H)-one (CTT), Langmuir isotherm.

### 1. INTRODUCTION

The fifth-most common metal on the planet, copper, is very beneficial both in its pure form and as an alloy [1]. Owing to their excellent properties such as good thermal and electrical conductivity, mechanical workability, low cost and high corrosion resistance, copper and its alloys were extensively used in various industries such as conductors, heat exchangers, and the electronic industry [2,3]. Copper has a relatively noble potential, despite this, it corrodes far more quickly in chloride and seawater conditions [4,5]. It is widely known that the amount of chloride ions in the environment affects how easily copper dissolves anodically. The formed  $\text{CuCl}$ , which is not sufficiently protective, and dissolves when it reacts with excess chloride [6–8]. In spite of its high corrosion resistance feature in atmospheric conditions, by forming an

oxide protective layer on its surface, copper and its alloys may easily undergo metal dissolution in the presence of an aggressive media like chloride having environment [6]. The primary technique for protecting metals and alloys is the use of inhibitors. Right now, green inhibitors show promise since they provide effective inhibition while having a minimal negative impact on the environment. Several investigators have reported [5–8] that organic compounds can act as possible corrosion inhibitors for numerous metals and alloys in various corrosive media. The inhibitors can be introduced to the medium or coated on the metal surface to slow down the corrosion process to avoid corrosion in the metal used in such corrosive media; both methods work well [9–13]. Heterocyclic compounds having N, O, S, P, or  $\pi$ -bonds make up many effective corrosion inhibitors by generating a physical barrier to reduce the transport of corrosive species to the metal surface [14–16].

Organic compounds that include conjugated double bonds and hetero atoms especially those, that can form polymeric complexes with copper by coordinating with  $\text{CuO}$ ,  $\text{Cu}^+$ , or  $\text{Cu}^{2+}$  through their

\*Corresponding author: Abd El-Aziz S. Fouda

E-mail: [asfouda@mans.edu.eg](mailto:asfouda@mans.edu.eg)

Paper received: 03. 01. 2024.

Paper accepted: 16. 02. 2024.

Paper is available on the website: [www.idk.org.rs/journal](http://www.idk.org.rs/journal)

lone pair electrons [17]. These adhere to the copper surface to produce a protective coating that prevents corrosion by serving as a wall against harmful ions like chloride [18]. 1,2,3-triazole (BTA) compound has been reported as a well-known effective corrosion inhibitors of copper in many environments [19]. The inhibition effect of 3-amino-1,2,4-triazole (ATA) on copper corrosion in 2M HNO<sub>3</sub> solution was studied by Zarrouk et al [20]. The inhibition efficiency reached 82.2% at 10-2M. Yaroslav et al [21] studied the protection of steels with a 3-substituted 1,2,4-triazole (3ST) in 2 M H<sub>2</sub>SO<sub>4</sub> solution. The inhibition protection reached 97.8% at 4.2x10<sup>-7</sup>M. Additionally, the ability of some 1,2,4-triazole derivatives to suppress copper corrosion in a neutral aqueous environment has been investigated. These derivatives include 3-vanilidene amino 1,2,4-triazole phosphonate, 3-anisalidene amino 1,2,4-triazole phosphonate [22], and 3-amino-5-mercapto-1,2,4-triazole [23, 24]. 1,2,4-triazole derivatives, including 1,2,4-triazole, 3-amino-1,2,4-triazole, and 2-4-diamino-1,2,4-triazole in 1 M H<sub>2</sub>SO<sub>4</sub> [25]; 3,5-bis(2-thienyl)-4-amino-1,2,4-triazole in 1 M HCl and 0.5 M H<sub>2</sub>SO<sub>4</sub> [26,27]; 3,5-diamino-1,2,4-triazole in 2 M HNO<sub>3</sub> [28]; 5-amino-1,2,4 triazole, 5-amino-3-mercapto 1,2,4 triazole, 5-amino-3-methyl thio-1,2,4-triazole, 1-amino-3-methyl thio-1,2,4-triazole [29–33]; 4-amino-4H-1,2,4-triazole-3-thiol, 4-amino-5-methyl-4H-1,2,4-triazole-3-thiol [34, 35] in 0.5 M HCl have been studied in relation to copper corrosion. Chooto et al [36] reported the effect of thioureas and N, O, S-Ligating Ring Compounds as corrosion inhibitors for Cu in Cl<sup>-</sup> ions. Wang et al. [37] investigate the inhibition mechanism of combined thiourea and hexamethylenetetramine as a corrosion inhibitor on the surface of copper in 0.5 M HCl solution.

With the improvement of hardware and software, recently, quantum chemical methods like functional density theory (DFT) has been used as fast and powerful tool to predict and understand corrosion inhibition performances of inhibitors [38]. Although there is an extensive literature on the corrosion properties of benzotriazole on steel and copper [39, 40], a protective coating is created by utilizing a tiny inhibitor dose to delay the corrosion reaction [41-43].

The organ-sulphur and heterocyclic compounds have the basic requirements to be considered as eco-friendly compounds. These compounds are adsorbed on the metal surface by blocking the active sites during the inhibition process. This leads to the need of development of new environmentally-friendly inhibitors for copper metal. A newly synthesized 3-(4-chlorophenyl)-7-methyl-5H-[1,2,4]triazolo[3,4-b][1,3,4]thiadiazin-6(7H)-one

one, was investigated for its ability to suppress the corrosion of copper in one molar HNO<sub>3</sub>. The evaluation of the corrosion behavior of copper in aggressive media in the absence and presence of newly synthesized CTT using (PDP), (EIS), and ML methods were discussed".

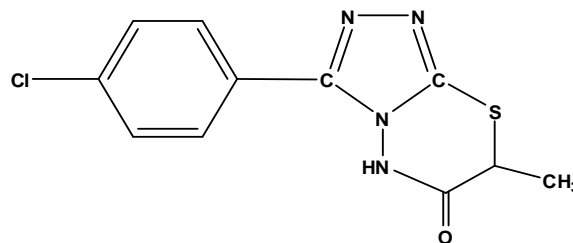
## 2. EXPERIMENTAL

### 2.1. Solutions and materials

The chemical composition of the Cu used in this paper is as follows: "(wt. %) 0.0023 Zn, 0.0023 Pb, 0.0023 P, 0.0019 Co, 0.0018 Al, 0.0015 Si, 0.004 Ni and the remainder is copper. Copper samples of measured (2 x 2 x 0.2) cm in triplicate, were mechanically polished. Samples were abraded with emery paper of grades levels from 250 and until 1200, then cleaned by distilled water, brushed using acetone and at end dried by filter papers. The strong solutions (5 M HNO<sub>3</sub>) were prepared by diluting AR grade (70 %) HNO<sub>3</sub> with bi-distilled water and checking its concentration with standardized solution of NaOH, after that prepare one molar HNO<sub>3</sub> by diluting with bi-distilled water. 100 mL stock solutions (10<sup>-3</sup> M) were prepared by dissolving an accurately weighed quantity of CTT in an appropriate volume of dimethyl formamide (DMF) and absolute ethanol, then diluting with bi-distilled water to the needed concentrations (4x10<sup>-6</sup> - 24 x10<sup>-6</sup> M).

### 2.2. Synthesis of 3-(4-chlorophenyl)-7-methyl-5H-[1,2,4]triazolo[3,4-b][1,3,4]thiadiazin-6(7H)-one [44].

The chemical structure and molecular formula of the 3-(4-chlorophenyl)-7-methyl-5H-[1,2,4]triazolo[3,4-b][1,3,4]thiadiazin-6(7H)-one (CTT) compound was shown in Figure 1. The studies were done at different concentrations (4x10<sup>-6</sup>, 8x10<sup>-6</sup>, 12x10<sup>-6</sup>, 16x10<sup>-6</sup>, 20x10<sup>-6</sup> and 24x10<sup>-6</sup> M) on the presence and absence of the investigated CTT. In thermostatic conditions, all experiments were conducted.



**3-(4-chlorophenyl)-7-methyl-5H-[1,2,4]triazolo[3,4-b][1,3,4]thiadiazin-6(7H)-one**

Figure 1 Optimized structure of CTT, (C<sub>11</sub>H<sub>9</sub>ClN<sub>4</sub>OS), M. Wt. = 280.02 g/mol

Slika 1 Optimizovana struktura CTT, (C<sub>11</sub>H<sub>9</sub>ClN<sub>4</sub>OS), M. Vt. = 280.02 g/mol

### 2.3. ML method

Specimens with emery paper were abraded, and bi-distilled water was used to clean it, then using filter papers for drying and weighed. In the existence and absence of various amounts of CTT, the samples were immersed into 100 mL of the acid medium. The CTT doses were between  $1 \times 10^{-6}$ – $24 \times 10^{-6}$  M. The time of immersion is 30 to 180 minutes. After a certain time, the samples were weighed again. The corrosion rate ( $k_{\text{corr}}$ ) of the metal specimens was determined using the following relationship” [45].

$$CR = \frac{\Delta W}{AT} \quad (1)$$

Where,  $\Delta W$  (mg) as the reduction in mass,  $A$  ( $\text{cm}^2$ ) as the area of the surface of Cu and  $t$  (min) as the time. The protection efficacy (% IE) in addition to specimen surface coverage ( $\Theta$ ) by CTT can be obtained as follows”:

$$\% IE = \theta \times 100 = \left( \frac{\Delta W_2 - \Delta W_1}{\Delta W_2} \right) \times 100 \quad (2)$$

with  $\Delta W_1$  as ML in the presence of the CTT and  $\Delta W_2$  as ML in the absence of the CTT.

### 2.4. Electrochemical techniques

For the electrochemical experiments, a standard electrochemical cell made-up from Pyrex glass was used. Cu ( $1 \text{ cm}^2$  exposed area) as working electrode, a saturated calomel electrode (SCE) and a platinum sheet as reference, and counter electrodes, respectively were used for electrochemical studies. Potentiodynamic current-potential graphs were documented by instantaneously shifting the electrode potential from  $-700 \text{ mV}$  to  $+700 \text{ mV}$  at a scanning rate of  $0.2 \text{ mVs}^{-1}$  (version 3.20). Corrosion current density ( $i_{\text{corr}}$ ) and corrosion potential ( $E_{\text{corr}}$ ) were assessed from the relationship of the correlation anodic and cathodic sections of Tafel plots in the absence and existence of various inhibitor doses. Before initiating the readings, the electrode potential was stabilized for 30 minutes. Gamry reference PCI300/4 Potentiostat/Galvanostat/Zra analyzer, DC105 corrosion, EIS300, Echem Analyst 5.5 software's were used for result plotting, graphing, data fitting, and calculating. The results of every experiment were checked at least three times. The degree of surface coverage ( $\theta$ ), and % IE were calculated using Eq. 3:

$$\% IE = \theta \times 100 = \left( \frac{i_{\text{corr}}(\text{free}) - i_{\text{corr}}(\text{inh})}{i_{\text{corr}}(\text{free})} \right) \times 100 \quad (3)$$

Where, “ $i_{\text{corr}}(\text{inh})$  and  $i_{\text{corr}}(\text{free})$  to indicate the currents densities in absence and existence of CTT, individually”.

For impedance calculation, open circuit potential (OCP) has been applied and current signals range from 100 kHz to 10 Hz. The  $\theta$  and % IE were calculated as follows:

$$\% IE_{EIS} = \left( \frac{R_{\text{ct}}^*(\text{inh}) - R_{\text{ct}}(\text{free})}{R_{\text{ct}}(\text{inh})} \right) \times 100 \quad (4)$$

with  $R_{\text{ct}}(\text{free})$  as the resistance in blank solution and  $R_{\text{ct}}(\text{inh})$  as the resistance of charge transfer in inhibited solution.

### 2.5. Surface morphology by SEM and EDX techniques

The specimens were placed in one molar  $\text{HNO}_3$  solution for 24 hours, both with and without higher doses of CTT ( $24 \times 10^{-6}$  M), after preparing their surfaces as before, then examined by Scanning electron microscope (SEM, JSM-T20, Japan) for the test. Furthermore, the copper samples were examined using energy dispersive X-ray (EDX) spectroscopy system provided (Zeiss Evo 10 instrument model)”. The beam accelerating voltage was 25 kV.

### 2.6. Computational chemical approaches

To study the relationship among the molecular structure and the reactivity of CTT, The density functional theory (DFT) in Materials Studio version 7.0 was utilized for theoretical computations.

## 3. RESULT AND DISCUSSION

### 3.1. ML tests

The ML of Cu in the acid environment at “ $25^\circ\text{C}$  without and in presence of altered doses of CTT after several immersion periods from 30 to 180 min is given in Figure 2.

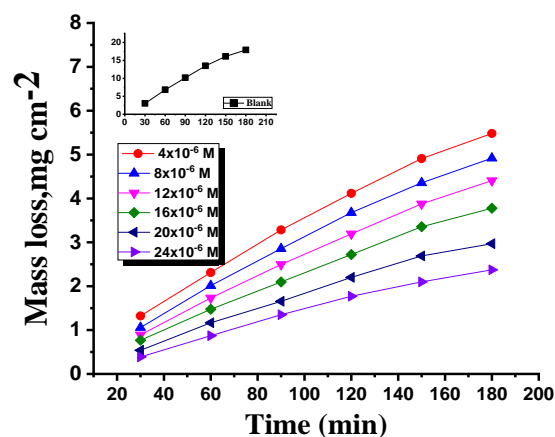


Figure 2. ML-Time diagrams at  $25^\circ\text{C}$  for the dissolution process of the Cu in one molar nitric acid in the absence and at various doses of CTT

Slika 2. ML-vremenski dijagrami na  $25^\circ\text{C}$  za proces rastvaranja Cu u jednoj molarnoj azotnoj kiselini u odsustvu i pri različitim dozama CTT-a

The ML was decreased as the CTT concentration increases. This due to the layer formed on the Cu surface from the adsorbed molecules of CTT which protects Cu surface from the corrosive environment and blocks the metal corrosive sites [46]. According to the data, the %IE value climbed to 85.9% as the CTT concentration was raised from the range of  $4 \times 10^{-6}$  to  $24 \times 10^{-6}$  M. The Cu outer surface area was sufficiently protected from corrosion when the  $k_{corr}$  declined and the CTT concentration grew. When the CTT level was raised from  $4 \times 10^{-6}$  to  $24 \times 10^{-6}$  M, the  $k_{corr}$  reduced from 0.0498 to 0.0237  $\text{mg cm}^{-2} \text{min}^{-1}$ . It was observed that the % IE dropped after  $24 \times 10^{-6}$  M. This decrease is probably caused by the CTT

molecules saturating every active area on the Cu surface [47].

### 3.1.1. Impact of temperature

Corrosion rate ( $k_{corr}$ ) of Cu,  $\theta$  and % IE at various temperatures in the acid environment in the absence and at various doses of CTT were presented in Table 1. The ( $k_{corr}$ ) decreased while  $\theta$  and % IE improved with increased doses of CTT. % IE decreased by raising the temperature due to desorption process [48] illustrating that the CTT is physically adsorbed on the Cu surface. The impact of temperature on the desorption process on the metal surface was covered in earlier research [49].

Table 1. CR,  $\theta$  and percent IE at various temperatures for corrosion of the Cu in the used acid medium in the absence and at various doses of CTT compound

Tabela 1. CR,  $\theta$  i procenat IE na različitim temperaturama za koroziju Cu u korišćenom kiselom medijumu u odsustvu i pri različitim dozama CTT jedinjenja

Temp, °C	(30°C)			(35°C)			(40°C)			(45°C)		
Conc., M	$k_{corr}$	$\theta$	IE %	$k_{corr}$	$\theta$	IE %	$k_{corr}$	$\theta$	IE %	$k_{corr}$	$\theta$	IE %
0.0	0.1683	---	---	0.2198	---	---	0.2848	---	---	0.3285	---	---
$4 \times 10^{-6}$	0.0498	0.704	70.4	0.0736	0.665	66.5	0.1213	0.574	57.4	0.1679	0.489	48.9
$8 \times 10^{-6}$	0.0449	0.733	73.3	0.0675	0.693	69.3	0.1170	0.589	58.9	0.1544	0.53	53.0
$12 \times 10^{-6}$	0.0402	0.761	76.1	0.0589	0.732	73.2	0.1054	0.63	63.0	0.1386	0.578	57.8
$16 \times 10^{-6}$	0.0340	0.798	79.8	0.0543	0.753	75.3	0.0883	0.69	69.0	0.1225	0.69	62.7
$20 \times 10^{-6}$	0.0279	0.834	83.4	0.0459	0.791	79.1	0.0783	0.725	72.5	0.1061	0.725	67.7
$24 \times 10^{-6}$	0.0237	0.859	85.9	0.0385	0.825	82.5	0.0720	0.747	74.7	0.0910	0.747	72.3

The following Arrhenius equation was used to estimate activation energy ( $E_a$ ):

$$\log k_{corr} = \left( \frac{-E_a^*}{2.303RT} \right) + \log A \quad (5)$$

where A as (pre-exponential Arrhenius multiplier), R (8.314 Joule/ K. mol.) as universal gas constant. Figure 3 indicates Arrhenius plots without and with various dose of CTT for Cu corrosion in the used acid medium. Results of  $E_a^*$  were determined from the lines slope. Enthalpy ( $\Delta H^*$ ) and entropy ( $\Delta S^*$ ) of the activation process can be specified by application the transition state equation as follows:

$$\log k_{corr} = \log \left( \frac{R}{Nh} \right) + \frac{\Delta S^*}{2.303R} + \frac{\Delta H^*}{2.303RT} \quad (6)$$

With h ( $6.625 \times 10^{-27}$ ) as Planck's constant and N ( $6.025 \times 10^{23}$  g/mol.) as Avogadro's number. Figure 4 displays  $\log(k_{corr}/T)$  against  $(1/T)$  diagrams without and with various doses of CTT for Cu corrosion in the used acid medium. Slopes and intercepts of the straight lines give values  $\Delta H^*$  and  $\Delta S^*$ , respectively. The determined activation parameters were depicted in Table 2. Values of  $E_a^*$  in Table 2 for solutions with CTT were high than that in its absence. The rise in the  $E_a^*$  shows that CTT molecules are physically adsorbed on the Cu surface. The exothermic activation process was

demonstrated by the negative sign of  $\Delta H^*$  values. This proves that the Cu dissolution in the acid medium is a unimolecular reaction. The negative signals of  $\Delta S^*$  showed that the disorder develops along the direction from the reactant to the activated complex [50].

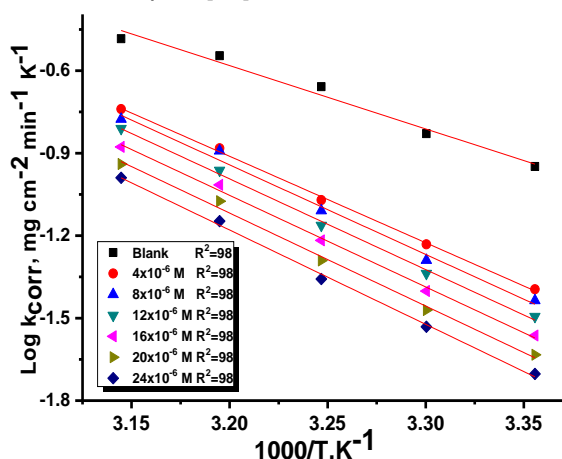


Figure 3.  $\log k_{corr}$  against  $1/T$  diagrams without and at various doses of CTT for Cu corrosion in the used acid medium

Slika 3.  $\log k_{corr}$  naspram  $1/T$  dijagrama bez i pri različitim dozama CTT za koroziju Cu u korišćenom kiselom medijumu.

Table 2. Thermodynamic activation parameters without and at various doses of CTT for Cu corrosion in the used acid medium

Tabela 2. Parametri termodinamičke aktivacije bez i pri različitim dozama CTT za koroziju Cu u korišćenom kiselom mediju

Conc. M	Activation parameters		
	E <sub>a</sub> <sup>*</sup> kJ mol <sup>-1</sup>	-ΔH <sup>*</sup> kJ mol <sup>-1</sup>	-ΔS <sup>*</sup> J mol <sup>-1</sup> K <sup>-1</sup>
Blank	45.2	41.6	122.1
4x10 <sup>-6</sup>	61.5	58.9	77.0
8x10 <sup>-6</sup>	63.6	61.0	70.8
12x10 <sup>-6</sup>	64.4	62.0	69.1
16x10 <sup>-6</sup>	65.1	62.5	68.3
20x10 <sup>-6</sup>	66.0	63.4	66.4
24x10 <sup>-6</sup>	66.9	64.3	64.6

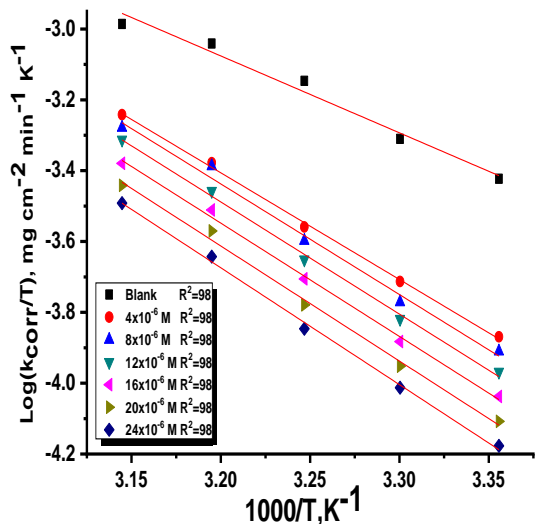


Figure 4. log (k<sub>corr</sub>/T) against 1/T diagrams without and at various doses of CTT for Cu corrosion in the used acid medium

Slika 4. log (k<sub>corr</sub>/T) naspram 1/T dijagrama bez i pri različitim dozama CTT-a za koroziju Cu u korišćenom kiselom mediju

3.1.2. Adsorption studies

The Langmuir model's isotherm for adsorption perfectly match the data (Figure 5). The following Eq. 7 can be used to show the Langmuir adsorption isotherm.

$$\frac{C_{inh}}{\theta} = \frac{1}{K_{ads}} + C_{inh} \tag{7}$$

with C as the dose of CTT inhibitor and K<sub>ads</sub> as the adsorption constant. Eq. 8 can be applied to give the free energy of adsorption (ΔG<sup>o</sup><sub>ads</sub>):

$$K_{ads} = \frac{1}{55.5} \exp\left(\frac{-\Delta G_{ads}^o}{RT}\right) \tag{8}$$

where the water dose at the Cu/solution interface is 55.5 (mol./L). By using the Vant Hoff equation, the enthalpy of adsorption (H<sup>o</sup><sub>ads</sub>) was determined as follows:

$$\log K_{ads} = \frac{-\Delta H_{ads}^o}{2.303RT} + constant \tag{9}$$

Figure 6 indicates draw among 1/T and log K<sub>ads</sub>. From the line slope, ΔH<sup>o</sup><sub>ads</sub> value can be determined. ΔS<sup>o</sup><sub>ads</sub> can be gotten by applying the next balance:

$$\Delta S_{ads}^o = \frac{\Delta H_{ads}^o - \Delta G_{ads}^o}{T} \tag{10}$$

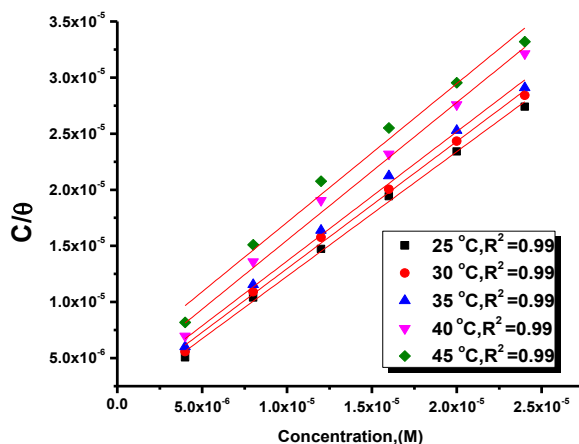


Figure 5. Langmuir adsorption plots of CTT on Cu surface at different temperatures

Slika 5. Langmuir-ovi adsorpcioni grafikoni CTT na površini Cu pri različitim temperaturama

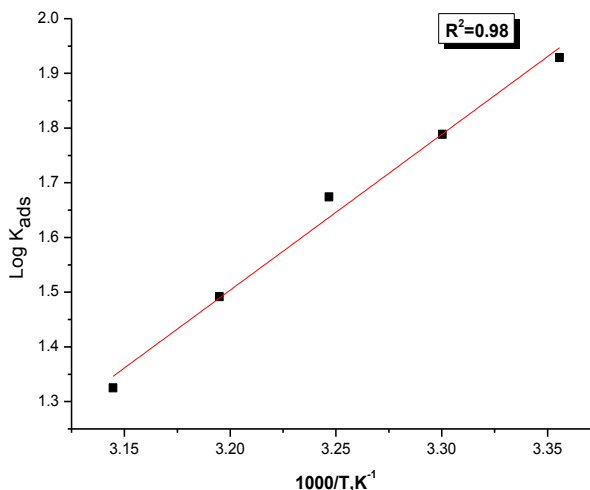


Figure 6. log K<sub>ads</sub> against 1/T for adsorption of CTT on Cu surface

Slika 6. log K<sub>ads</sub> prema 1/T za adsorpciju CTT na površini Cu

The negative value of ΔG<sup>o</sup><sub>ads</sub> indicates the spontaneity and the stability of the CTT adsorption layer occurred on the Cu surface (Table 3). The

obtained values of  $\Delta G_{\text{ads}}^{\circ}$ , are around  $20 \text{ kJ mol}^{-1}$  indicates the physisorption of the CTT molecules on the Cu surface. Indicating that the adsorption procedure is exothermic this obtained from the negative values of  $\Delta H_{\text{ads}}^{\circ}$ .

Table 3. Adsorption parameters for CTT at different temperatures

Tabela 3. Parametri adsorpcije za CTT na različitim temperaturama

Temp. °C	$K_{\text{ads}}$ M <sup>-1</sup>	$-\Delta G_{\text{ads}}^{\circ}$ kJ mol <sup>-1</sup>	$-\Delta H_{\text{ads}}^{\circ}$ kJ mol <sup>-1</sup>	$-\Delta S_{\text{ads}}^{\circ}$ J mol <sup>-1</sup> K <sup>-1</sup>
25	85	20.9	54.0	70.1
30	61	20.4		67.4
35	47	20.1		65.2
40	31	19.3		61.7
45	21	18.7		58.5

Table 4. PP parameters for liquefaction of the Cu in the used acid environment without and at altered doses of CTT

Tabela 4. PP parametri za tečenje Cu u korišćenju kiseloj sredini bez i pri izmenjenim dozama CTT

Conc. M	$i_{\text{corr}}$ , $\mu\text{A cm}^{-2}$	$-E_{\text{corr}}$ , mV vs SCE	$\beta_a$ mV dec <sup>-1</sup>	$-\beta_c$ mV dec <sup>-1</sup>	C.R, 10 <sup>2</sup> mpy	$\Theta$	% IE
Blank	396	19	115	185	381	--	--
$4 \times 10^{-6}$	244	23	111	177	272	0.384	38.4
$8 \times 10^{-6}$	157	14	113	191	153	0.604	60.4
$12 \times 10^{-6}$	142	19	109	187	149	0.641	64.1
$16 \times 10^{-6}$	137	25	99	197	147	0.654	65.4
$20 \times 10^{-6}$	103	26	88	201	58	0.740	74.0
$24 \times 10^{-6}$	39	24	93	174	25	0.902	90.2

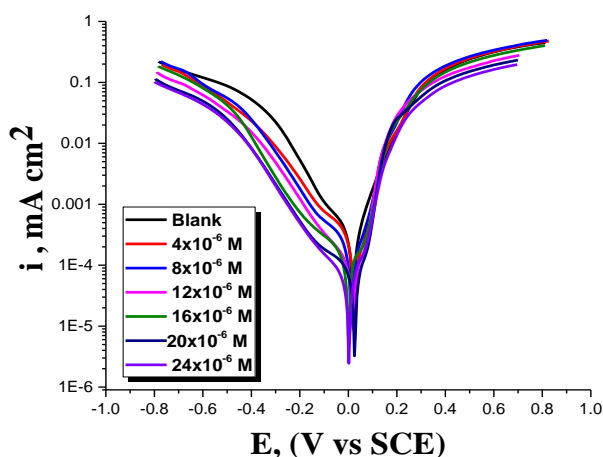


Figure 7. PDP curves for corrosion of the Cu in the used acid medium without and at various doses of CTT

Slika 7. PDP krive za koroziju Cu u korišćenju kiseloj sredini bez i pri različitim dozama CTT

### 3.2. Electrochemical Techniques

#### 3.2.1. PDP tests

PDP curves in the absence and at different doses of CTT for Cu in the acid medium were presented in the Figure 7. It is apparent that the examined CTT retards the anodic dissolution of Cu and cathodic discharge of oxygen. PDP results such as ( $E_{\text{corr}}$ ), ( $i_{\text{corr}}$ ), slopes of Tafel lines ( $\beta_a$  and  $\beta_c$ ),  $\theta$ , and % IE were determined and tabulated in Table 4. Lowering the values of  $i_{\text{corr}}$  is because the CTT has been adsorbed on the surface of the Cu. There is no clear change in  $E_{\text{corr}}$ ,  $\beta_a$  and  $\beta_c$  in the protect solutions associated with the uninhibited one, and there is no definite change in data of  $E_{\text{corr}}$ , these indicate that the CTT behaves as mixed kind inhibitor [51]. In addition, cathodic slope ( $\beta_c$ ) moved to more negative direction and the anodic slope ( $\beta_a$ ) moved to more positive direction in presence of the CTT inhibitor. The parallel Tafel lines indicate that the mechanism of the corrosion reaction is preserved and the basic adsorption mode prevents the corrosion reaction [52].

#### 3.2.2. EIS tests

For the Cu electrode, Nyquist plots were produced in the presence and at different doses of CTT at their respective corrosive potential after 30 minutes of immersion in the acid medium. Figure 8 shows the resulting Nyquist and Bode plots. It is clear that the inductive loops in the blank solution are bigger when the CTT is present than when it is not, and that the size increases in direct proportion to the concentration of CTT [53]. Interestingly, the frequency dispersion effect causes the capacitive loops to diverge from perfect semicircles. The applied electrical circuit model equivalent for fitting EIS results was displayed in Figure 9, it explains the resistance of charge transfer ( $R_{\text{ct}}$ ) values, constant phase element (CPE), resistance of solution ( $R_s$ ) and quadratic resistance ( $W_d$ ). The data in Table 5 include resistance ( $R_{\text{ct}}$ ) to charge transfer, capacitance ( $C_{\text{dl}}$ ) of double layer, ( $\Theta$ ) and (%IE) attained from EIS test. As the CTT dose is

increased, it is shown that  $R_s$  and  $R_{ct}$  values rise but  $C_{dl}$  values decrease; it may be demonstrated by exchange between the molecules of the water and

the CTT molecule which adsorb on the metal's surface and/or increasing the double layer thickness [54].

Table 5. EIS parameters for Cu corrosion in the used acid medium without and at various doses of CTT

Tabela 5. EIS parametri za Cu koroziju u korišćenom kiselom medijumu bez i pri različitim dozama CTT

Conc., M	$R_{ct}$ , $\Omega \text{ cm}^2$	$C_{dl}, \times 10^{-3} \mu\text{F cm}^{-2}$	$\theta$	%IE
Blank	23	142	---	---
$4 \times 10^{-6}$	76	123	0.697	69.7
$8 \times 10^{-6}$	102	101	0.775	77.5
$12 \times 10^{-6}$	208	76	0.889	88.9
$16 \times 10^{-6}$	220	68	0.895	89.5
$20 \times 10^{-6}$	245	51	0.906	90.6
$24 \times 10^{-6}$	270	37	0.915	91.5

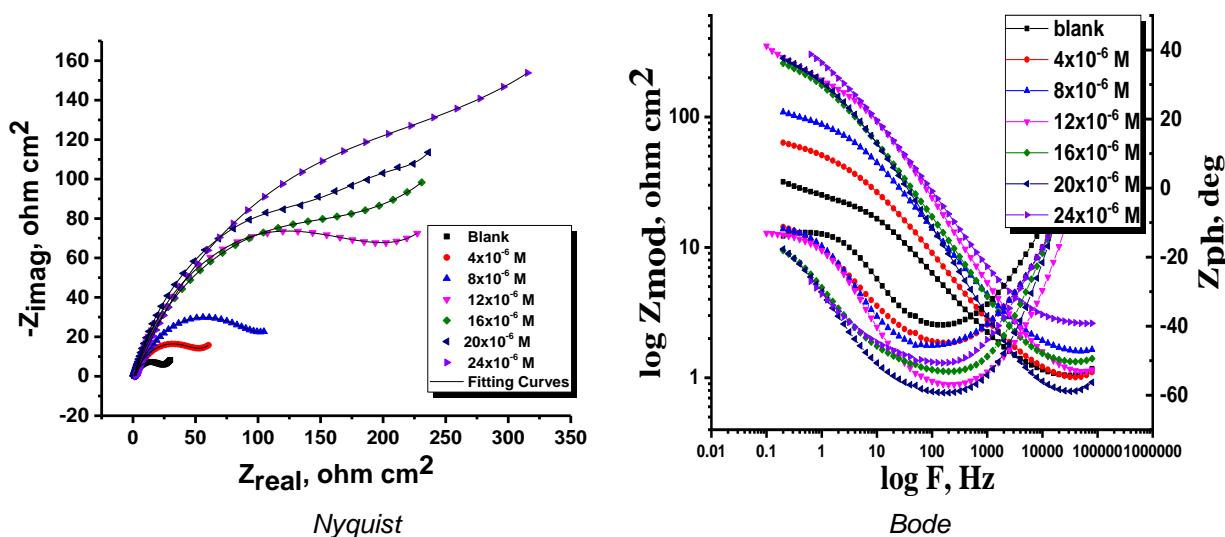


Figure 8. Nyquist and Bode graphs for Cu corrosion in the used acid medium without and at various doses of CTT

Slika 8. Nyquist i Bode-ov grafikon za koroziju Cu u korišćenom kiselom medijumu bez i pri različitim dozama CTT-a

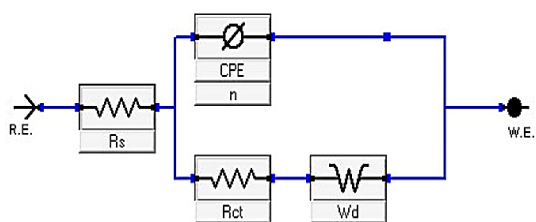


Figure 9. The circuit used to analyze the EIS values

Slika 9. Kolo koje se koristi za analizu EIS vrednosti

### 3.3. Surface examinations

#### 3.3.1. SEM analysis

SEM analysis was performed on the Cu surface to determine whether the surface

morphology was changed when a specific concentration of CTT molecules was used. SEM micrographs obtained for Cu samples without and with  $24 \times 10^{-6}$  M CTT presented in Figure 10. When the tested inhibitor was present, it significantly reduced Cu surface corrosion as seen in Figure 10b and the Cu surface was smooth. In the absence of any inhibitor, corrosion significantly weakened the Cu's surface in  $\text{HNO}_3$  (Figure 10a), resulting in visible pits and cavities [55]. We can deduce from the SEM results that when the inhibitor was utilized, a protective coating formed on the Cu superficial [56]. According to EDX analysis, the Cu surface is heavily damaged without the inhibited solution, where the images of inhibited Cu surface indicated less corrosion in the presence of examined inhibitors. Also, the percentage of iron in the Cu surface immersed in

inhibited solution is decreasing, while the percentage of the carbon and heteroatoms (S, O and N) is increasing. From the SEM-EDX tests, we can conclude that the examined CTT adsorbed on

the Cu metal surface shows an excellent image for preventing severe corrosion of the metal surface [57].

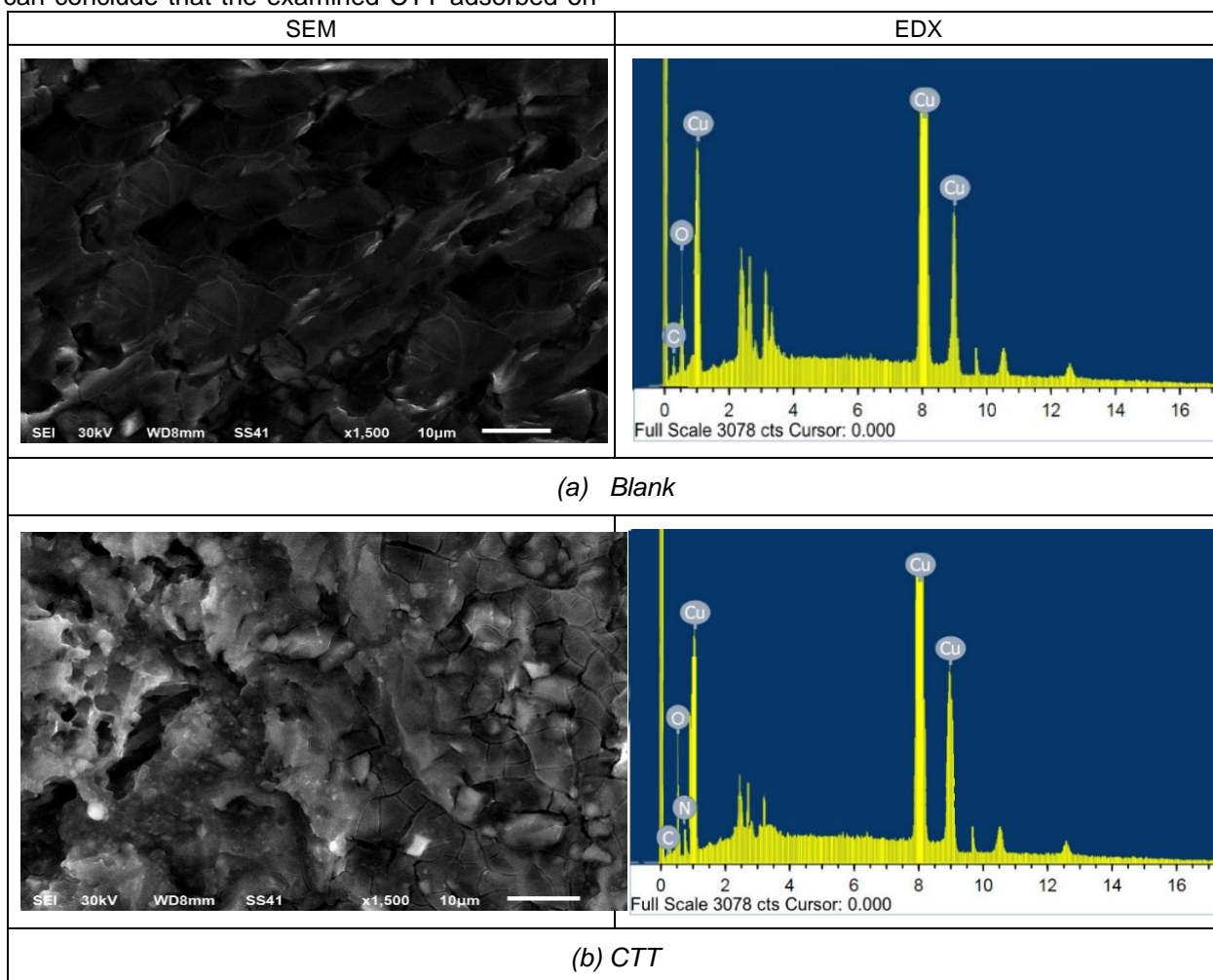


Figure 10. SEM and EDX profiles for: (a) After of 24-hour immersion in  $\text{HNO}_3$  (1.0 M), (b) with  $24 \times 10^{-6}$  M CTT presented

Slika 10. SEM i EDX profili za: (a) Posle 24-časovnog potapanja u  $\text{HNO}_3$  (1,0 M), (b) sa prikazanim CTT  $24 \times 10^{-6}$  M

### 3.4. Quantum Chemical Parameters

The highest ( $E_{\text{HOMO}}$ ) occupied value of a molecule represents its ability to donate two unshared electrons. On the other hand, a larger  $E_{\text{HOMO}}$  indicates a greater likelihood that the molecule will provide protons to an electroscopic reagent [58]. A higher propensity for the molecule to absorb electrons from the metal atoms is shown by a lower energy of the empty molecular orbital ( $E_{\text{LUMO}}$ ). The energy band gap  $\Delta E_g$  ( $\Delta E = E_{\text{HOMO}} - E_{\text{LUMO}}$ ) that the lower energy gap values are reflected to be great reactivity of the CTT molecule and have excellent corrosion behavior onto the Cu surface [59]. Different parameters were resulted via the calculations. The quantum parameters connotation with corrosion hindrance were

calculated containing ionization potential ( $I_p = -E_{\text{HOMO}}$ ), molecular dipole moment ( $\mu$ ), electron affinity ( $E_A = -E_{\text{LUMO}}$ ), global hardness ( $\eta$ ), electronegativity ( $\chi$ ) that are used to calculate the electrons transfer from the inhibitor molecule to the metallic atom  $\Delta N$ , electrophilicity index ( $\omega$ ), softness ( $\sigma$ ), and back-donation ( $\Delta E$  back-donation)", were calculated as Koopmans's theorem" [60] from the next balance:

$$\mu = -\chi = -\frac{I_p + E_A}{2} \quad (11)$$

$$\chi = \frac{I_p + E_A}{2} \quad (12)$$

$$\eta = \frac{I_p - E_A}{2} \quad (13)$$



$$\sigma = \frac{1}{\eta} \quad (14)$$

$$\omega = \frac{\mu^2}{2\eta} \quad (15)$$

$$\Delta E_{back\ donation} = -\frac{\eta}{4} \quad (16)$$

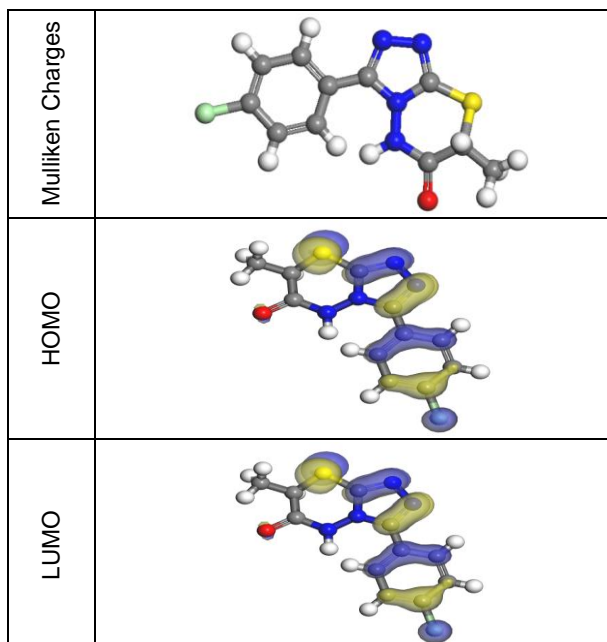


Figure 10 The electron density maps of HOMO and LUMO for the CTT Vilazodone are provided by the frontier molecular

Slika 10 Mape elektronske gustine HOMO i LUMO za CTT Vilazodon su obezbeđene od strane graničnog molekula

A molecule's polarity is determined by its molecular dipole moment ( $\mu$ ) [61]. A higher degree of polarization in the molecule is associated with a larger dipole moment. A recent research [62] claims that higher dipole moment levels and lower  $\Delta E$  values both enhance % IE.

Table 6. Quantum statistics for the considered CTT inhibitor

Tabela 6. Kvantna statistika za razmatrani CTT inhibitor

Compound	CTT
$E_{HOMO}$ , eV	-5.386
$E_{LUMO}$ , eV	-3.313
$\Delta E$ , eV	2.07
$I_p$ , eV	5.386
$E_A$ , eV	3.313
$\eta$ , eV	1.04
$\sigma$ , eV	0.96
$\mu$ , eV	4.349
Dipole moment (Debye)	4.254

### 3.4. Inhibition mechanism analysis

There are two adsorption kinds, they are: chemisorption and physisorption. Usually, physisorption procedure requirements the attendance of charged molecules and charged Cu surface, while, chemisorption process contains sharing electrons or transferring them from the molecules of the CTT to the d-orbital of iron forming coordinate bond. CTT has electronegative donor atom O, N and  $\pi$  electrons of the aromatic rings. Effective CTT adsorption on the surface of the Cu is caused by these electronegative donor atoms or  $\pi$  electrons of the aromatic rings, or both of them. [63]. The positively charge of Cu surface in aqueous acid environment [64]. An electrostatic attraction causes the protonated CTT (cationic) to adsorb on the negatively charged metal surface created by the adsorbed  $Cl^-$  ions on the Cu sample. The specimen Cu sample could adsorb the protonated molecules. The adsorption process results in the formation of a corrosion-inhibiting layer on the surface of the Cu. Remove water from the Cu surface, then protect it from corrosion.

### 4. CONCLUSIONS

- 3-(4-chlorophenyl)-7-methyl-5H-[1,2,4] triazolo [3,4-b] [1,3,4]thiadiazin-6(7H)-one (CTT) shows high inhibition efficiency for corrosion of the Cu in one molar  $HNO_3$  solutions.
- Langmuir adsorption isotherm was followed when CTT was adsorbed onto Cu surface. The process of the adsorption is physical adsorption.
- % IE increases as CTT dose increases and as the temperature decreases.
- According to PDP method, CTT inhibitor has cathodic and anodic inhibitory effects.
- $C_{dl}$  decreases and  $R_{ct}$  increases as CTT concentration increased.
- Chemical and electrochemical tests showed that investigated CTT behaved as good corrosion inhibitor for Cu

### 5. REFERENCES

- X.J.Raj, N.Rajendran (2011) Corrosion inhibition effect of substituted thiadiazoles on brass. Int J Electrochem Sci.6(2), 348–66.
- S.Neupane, P.Losada-Pérez, U.Tiringer, P.Taheri, D.Desta, C.Xie (2021) Study of mercaptobenzimidazoles as inhibitors for copper corrosion: down to the molecular scale. J Electrochem Soc. 168(5), 51504. doi.org/10.1149/1945-7111/abf9c3
- C.U.Dueke-Eze, N.A.Madueke, N.B.Iroha, N.J. Maduelosi, L.A.Nnanna, V.C.Anadebe (2022) Adsorption and inhibition study of N-(5-methoxy-2-hydroxybenzylidene) isonicotinohydrazide Schiff base on copper corrosion in 3.5% NaCl. Egypt J Pet. 31(2), 31–7. doi.org/10.1016/j.ejpe.2022.05.001

- [4] A.S. Fouda, M.A. Ismail, M.A. Khaled, A. El-Hossiany (2022) Experimental and computational chemical studies on the corrosion inhibition of new pyrimidinone derivatives for copper in nitric acid. *Sci Rep.* 12(1), 16089. <https://doi.org/10.1038/s41598-022-20306-4>
- [5] E.M. Sherif, S.M. Park (2005) Inhibition of copper corrosion in 3.0% NaCl solution by N-phenyl-1, 4-phenylenediamine. *J Electrochem Soc.* 152(10), B428. [doi.org/10.1149/1.2018254](https://doi.org/10.1149/1.2018254)
- [6] S.H. Zaferani, M. Sharifi, D. Zaarei, M.R. Shishesaz (2013) Application of eco-friendly products as corrosion inhibitors for metals in acid pickling processes—A review. *J Environ Chem Eng.* 1(4), 652–657. [doi.org/10.1016/j.jece.2013.09.019](https://doi.org/10.1016/j.jece.2013.09.019)
- [7] M. Finšgara, I. Milošev, B. Pihlar (2007) Inhibition of Copper Corrosion Studied by Electrochemical and EQCN Techniques. *Acta Chim Slov.* 54(3), 591–597.
- [8] A. El Warraky, H.A. El Shayeb, E.M. Sherif (2004) Pitting corrosion of copper in chloride solutions. *Anti-Corrosion Methods Mater.* 51(1), 52–61. DOI: 10.1108/00035590410512735
- [9] S.H. Etaiw, G.S. Hassan, A.A. El-Hossiany, A.S. Fouda (2023) Nano-metal–organic frameworks as corrosion inhibitors for strengthening anti-corrosion behavior of carbon steel in a sulfuric acid environment: from synthesis to applications. *RSC Adv.* 13(22), 15222–35. [doi.org/10.1039/D3RA01644G](https://doi.org/10.1039/D3RA01644G)
- [10] M.B. Petrović Mihajlović, Ž.Z. Tasić, M.B. Radovanović, A.T. Simonović, M. Antonijević (2022) Electrochemical Analysis of the Influence of Purines on Copper, Steel and Some Other Metals Corrosion. *Metals (Basel)*. 12(7), 1150.
- [11] O.A.A. El-Shamy (2013) Effectiveness of some nonionic surfactants as corrosion inhibitors for carbon steel in hydrochloric acid solution. *Adv Mater Res.*, 787, 211–5. [doi.org/10.4028/www.scientific.net/AMR.787.211](https://doi.org/10.4028/www.scientific.net/AMR.787.211)
- [12] O.A.A. El-Shamy, M.A. Deyab (2023) Improvement of the corrosion resistance of epoxy coatings with the use of a novel zinc oxide-alginate nanoparticles compound. *Mater Lett.* 331, 133402. <https://doi.org/10.1016/j.matlet.2022.133402>
- [13] O.A.A. El-Shamy, M.A. Deyab (2023) Novel anti-corrosive coatings based on nanocomposites of epoxy, chitosan, and silver. *Mater Lett.* 330, 133298. <https://doi.org/10.1016/j.matlet.2022.133298>
- [14] A.M. Abdel-karim, R.A. Azzam, O. El-Said Shehata, M.A. Adly, O.A.A. El-Shamy, G.A. El Mahdy (2023) Synthesis of New Guanidine Benzothiazole Derivative and Its Application as Eco-Friendly Corrosion Inhibitor. *Egypt J Chem.* 66(7), 187–95. [doi.org/10.21608/EJCHEM.2022.167419.7063](https://doi.org/10.21608/EJCHEM.2022.167419.7063)
- [15] M.A. Deyab, O.A.A. El-Shamy, H.K. Thabet, A.M. Ashmawy (2023) Electrochemical and theoretical investigations of favipiravir drug performance as ecologically benign corrosion inhibitor for aluminum alloy in acid solution. *Sci Rep.* 13(1), 8680. [doi.org/10.1038/s41598-023-35226-0](https://doi.org/10.1038/s41598-023-35226-0)
- [16] A. Lachiri, M. El Faydy, F. Benhiba, H. Zarrok, M. El Azzouzi, M. Zertoubi (2018) Inhibitor effect of new azomethine derivative containing an 8-hydroxyquinoline moiety on corrosion behavior of mild carbon steel in acidic media. *Int J Corros Scale Inhib.* 7(4), 609–32. [doi.org/10.17675/2305-6894-2018-7-4-9](https://doi.org/10.17675/2305-6894-2018-7-4-9)
- [17] J. Saranya, F. Benhiba, N. Anusuya, R. Subbiah, A. Zarrouk, S. Chitra (2020) Experimental and computational approaches on the pyran derivatives for acid corrosion. *Colloids Surfaces A Physicochem Eng Asp.* 603, 125231. <https://doi.org/10.1016/j.colsurfa.2020.125231>
- [18] N.A. Madueke, N.B. Iroha (2018) Protecting aluminum alloy of type AA8011 from acid corrosion using extract from Allamanda cathartica leaves. *Int J Innov Res Sci Eng Technol.* 7(10), 10251–8. [doi.org/10.15680/IJRSET.2018.0710014](https://doi.org/10.15680/IJRSET.2018.0710014)
- [19] A.T. Simonović, Z.Z. Tasić, M.B. Radovanović, M.B. Petrović Mihajlović, M.M. Antonijević (2020) Influence of 5-chlorobenzotriazole on inhibition of copper corrosion in acid rain solution. *ACS omega.* 5(22), 12832–41. <https://doi.org/10.1021/acsomega.0c00553>
- [20] A. Zarrouk, B. Hammouti, H. Zarrok, M. Bouachrine, K.F. Khaled, S.S. Al-Deyab, (2012) Corrosion Inhibition of Copper in Nitric Acid Solutions Using a New Triazole Derivative, *Int. J. Electrochem. Sci.*, 7, 89 – 105. [https://doi.org/10.1016/S1452-3981\(23\)13323-2](https://doi.org/10.1016/S1452-3981(23)13323-2)
- [21] Y.G. Avdeev, A. Tatyana, A. Nenasheva, An. Yu. Luchkin, An. I. Marshakov, Y. I. Kuznetsov (2023) Thin 1,2,4-Triazole Films for the Inhibition of Carbon Steel Corrosion in Sulfuric Acid Solution, *Coatings*, 15(19), 6989. [doi.org/10.3390/ma15196989](https://doi.org/10.3390/ma15196989).
- [22] S Ramesh, S Rajeswari, S Maruthamuthu (2004) Corrosion inhibition of copper by new triazole phosphonate derivatives. *Appl Surf Sci*, 229, 214–225, <https://doi.org/10.1016/j.apsusc.2004.01.063>
- [23] J. Yu, L. Jiang, F. Gan (2010) Inhibition of copper corrosion in deionized water by 3-amino-5-mercapto-1,2,4-triazole. *J Chin Soc Corros Prot.* 30, 21–24. [doi.org/10.1016/j.apsusc.2004.01.063](https://doi.org/10.1016/j.apsusc.2004.01.063)
- [24] J. Yu, F. Gan, L. Jiang (2008) Inhibition effect of 3-amino-5-mercapto-1,2,4-triazole on copper corrosion. *Corrosion* 64, 900–904. [doi.org/10.5006/1.3294405](https://doi.org/10.5006/1.3294405)
- [25] A. Soumoue, B. El Ibrahimy, S. El Issami, L. Bazzi (2014) Some triazolic compounds as corrosion inhibitors for copper in sulphuric acid. *Int J Sci Res*, 3, 349–354.
- [26] Y.M. Tang, Y. Chen, Y. W. Zang, X.S. Yin, J.T. Wang (2010) 3,5-Bis(2-thienyl)-4-amino-1,2,4-triazole as a corrosion inhibitor for copper in acidic media. *Anti-Corros Methods Mater*, 57, 227–233
- [27] C. Y. hen, Y. Tang, W. Yang, Y. Liu, J. Wang (2009) Inhibition of 3,5-bis(2-thienyl)-4-amino-,2,4-triazole on copper in HCl media. *Corros Sci Prot Technol* 21, 406–409.
- [28] A. Zarrouk, B. Hammouti, S.S. Al-Deyab, R. Salghi, H. Zarrok, C. Jama, F. Bentiss (2012) Corrosion inhibition performance of 3,5-diamino-1,2,4-triazole for protection of copper in nitric acid solution. *Int J Electrochem Sci* 7, 5997–6011. [https://doi.org/10.1016/S1452-3981\(23\)19457-0](https://doi.org/10.1016/S1452-3981(23)19457-0)

- [29] A.Lalitha, S.Ramesh, S.Rajeswari (2005) Surface protection of carbon steel by hexanesulphonic acid-zinc ion system. *Electrochim Acta*, 51,47–55. 29. <https://doi.org/10.1155/2014/628604>
- [30] H.H.Hassan, E.Abdelghani, M.A.Amin (2007) Inhibition of mild steel corrosion in hydrochloric acid solution by triazole derivatives -Part I. *Electrochim Acta* 52, 6359–6364. <https://doi.org/10.1016/j.electacta.2007.08.021>
- [31] M.K.Awad, M.R.Mustafa, M.M.A.Elnga (2010) Computational simulation of the molecular structure of some triazoles as inhibitors for the corrosion of metal surface. *J Mol Struct (Theochem)*, 959, 66–74. <https://doi.org/10.1016/j.theochem.2010.08.008>
- [32] S.E.S.M.herif, R.M.Erasmus, J.D.Comins (2007) Effects of 3-amino-1,2,4-triazole on the inhibition of copper corrosion in acidic chloride solutions. *J Colloid Interface Sci*, 311,144–151. [doi.org/10.1016/J.JCIS.2007.02.064](https://doi.org/10.1016/J.JCIS.2007.02.064)
- [33] E.S.M.Sherif, R.M.Erasmus, J.D.Comins (2007) Corrosion of copper in aerated acidic pickling solutions and its inhibition by 3-amino-1,2,4-triazole-5-thiol. *J Colloid Interface Sci*,306, 96–104. [doi.org/10.1016/j.jcis.2007.01.003](https://doi.org/10.1016/j.jcis.2007.01.003)
- [34] P.Sudheer, M.A.Quraishi (2013) Electrochemical and theoretical investigation of triazole derivatives on corrosion inhibition behavior of copper in hydrochloric acid medium. *Corros, Sci*, 70,161–169. <https://doi.org/10.1016/j.corsci.2013.01.025>
- [35] E.G.Demissie, S.B.Kassa, G.W.Woyessa (2014) Quantum chemical study on corrosion inhibition efficiency of 4-amino-5-mercapto-1,2,4-triazole derivatives for copper in HCl solution. *Int J Sci, Eng Res*, 5, 304–312. [doi.org/10.14299/ijser.2014.06.001](https://doi.org/10.14299/ijser.2014.06.001)
- [36] Y.Wang, J.Hu, Y.Wang, Li.Yu (2016) A New Method for Preventing Corrosion Failure: Thiourea and Hexamethylenetetramine as Inhibitor for Copper, *Bull. Korean Chem. Soc.*, 37, 1797–1811. <https://doi.org/10.1002/bkcs.10978>
- [37] P. Chooto, W. Aemaek Tappachai, S. Duangthong, S. Manaboot (2020) Corrosion Inhibition of Copper by Thioureas, and N, O, S-Ligating Ring Compounds, *Port. Electrochim. Acta*, 38(5), 343-350. [doi.org/10.4152/pea.202005343](https://doi.org/10.4152/pea.202005343)
- [38] R.Vaira Vignesh, R.Padmanaban, M.Govindaraju (2020) Synthesis and characterization of magnesium alloy surface composite (AZ91D—SiO<sub>2</sub>) by friction stir processing for bioimplants. *Silicon*. 12(5),1085–102. <https://doi.org/10.1007/s12633-019-00194-6>
- [39] J. Liu, P.Hao, L.Jiang, L.Qian (2022) Novel Eco-friendly Slurries for Chemical Mechanical Polishing of GCr15 Bearing Steel. *Tribol Lett.* 70(3), 67-82. <https://doi.org/10.1007/s11249-022-01608-0>
- [40] H.Hussien, S.Shahen, A.M.Abdel-karim, I.M.Ghayad, O.A.A.El-Shamy, N.Mostfa (2023) Experimental and theoretical evaluations: Green synthesis of new organic compound bis ethanethioly oxalamide as corrosion inhibitor for copper in 3.5% NaCl. *Egypt J Chem.* 66(3),189–96. [doi.org/10.21608/ejchem.2023.182301.7364](https://doi.org/10.21608/ejchem.2023.182301.7364)
- [41] A.Fateh, M.Aliofkhazraei, A.R.Rezvanian (2020) Review of corrosive environments for copper and its corrosion inhibitors. *Arab J Chem.* 13(1),481–544. <https://doi.org/10.1016/j.jcis.2007.02.064>
- [42] A.M. Abdel-Karim, A.M.El-Shamy, Y. Reda (2022) Corrosion and stress corrosion resistance of Al Zn alloy 7075 by nano-polymeric coatings. *J Bio-and Tribo-Corrosion.* 8(2), 57. <https://doi.org/10.1007/s40735-022-00656-2>
- [43] B. Souad, S.Chafia, A.Hamza, M.Wahiba, B.Issam (2021) Synthesis, experimental and DFT studies of some benzotriazole derivatives as brass C68700 corrosion inhibitors in NaCl 3%. *Chemistry Select.* 6(6),1378–84. [doi.org/10.1002/slct.202004383](https://doi.org/10.1002/slct.202004383)
- [44] A.A. El-Barbary, A.Z.Abou-El-Ezz, A.A.Abdel-Kader, M.El-Daly, C.Nielsen (2004) Synthesis of some new 4-amino-1, 2, 4-triazole derivatives as potential anti-HIV and anti-HBV. *Phosphorus, Sulfur, and Silicon.* 179(8),1497–508. <https://doi.org/10.1080/10426500490463989>
- [45] E.E.Oguzie, C.Unaegbu, C.N.Ogukwe, B.N.Okolue, A.I.Onuchukwu (2004) Inhibition of mild steel corrosion in sulphuric acid using indigo dye and synergistic halide additives. *Mater Chem Phys.* 84(2–3),363–8. <https://doi.org/10.1016/j.matchemphys.2003.11.027>
- [46] P.Desai (2010) Efficiency of xlenol orange as corrosion inhibitor for aluminum in trichloroacetic acid. *Indian Journal of Chemical Technology*, 17, 50- 55, <https://ssrn.com/abstract=4234402>, <http://dx.doi.org/10.2139/ssrn.4234402>
- [47] A.M.Ayuba, A.Uzairu, G.A.Shallangwa (2018) Theoretical study of aspartic and glutamic acids as corrosion inhibitors on aluminum metal surface', *Moroccan, Journal of Chemistry*, 6(1), 6-12. [doi:10.48317/IMIST.PRSM/MORJCHEM-V6I1.9111](https://doi.org/10.48317/IMIST.PRSM/MORJCHEM-V6I1.9111)
- [48] S.A.Umoren, I.B.Obot, A.Madhankumar, Z.M.Gasem (2015) Performance evaluation of pectin as ecofriendly corrosion inhibitor for X60 pipeline steel in acid medium: Experimental and theoretical approaches' *Carbohydrate polymers*, 124, 280-291. [doi.org/10.1016/j.carbpol.2015.02.036](https://doi.org/10.1016/j.carbpol.2015.02.036)
- [49] Q.B.Zhang, Y.X.Hua (2009) Corrosion inhibition of mild steel by alkyimidazolium ionic liquids in hydrochloric acid', *Electrochim. Acta*, 54(6), 1881-1887. <https://doi.org/10.1016/j.electacta.2008.10.025>
- [50] N.Iroha, N.Maduelosi (2020) 'Pipeline steel protection in oil well acidizing fluids using expired pharmaceutical agent', *Chemistry International*, 6(4), 267-276. <https://ssrn.com/abstract=3693741>
- [51] P.Desai, S.M.Kapopara (2014) Inhibitory action of xlenol orange on aluminum corrosion in hydrochloric acid solution. *Indian Journal of Chemical Technology*, 21, 139-145. <https://ssrn.com/abstract=4234403> or <http://dx.doi.org/10.2139/ssrn.4234403>
- [52] P.S.Desai, R.T.Vahi (2011) Inhibitive efficiency of sulphathiazole for Alcorrosion in trichloroacetic acid. *Anti-Corrosion Methods Mater.* 58(2),70–75. <https://doi.org/10.1108/00035591111110714>
- [53] L.Larabi, Y.Harek, M.Traisnel, A.Mansri (2004) Synergistic influence of poly (4-vinylpyridine) and potassium iodide on inhibition of corrosion of mild steel in 1M HCl. *J Appl Electrochem.* 34, 833–9. <https://doi.org/10.1023/B:JACH.0000035609.09564.e6>

- [54] B.I.Ita, O.E.Offiong (2001) The study of the inhibitory properties of benzoin, benzil, benzoin-(4-phenylthiosemicarbazone) and benzil-(4-phenylthiosemicarbazone) on the corrosion of mild steel in hydrochloric acid. Mater Chem Phys. 70(3), 330–5. [https://doi.org/10.1016/S0254-0584\(00\)00476-4](https://doi.org/10.1016/S0254-0584(00)00476-4)
- [55] K.F.Khaled (2009) 'Monte Carlo simulations of corrosion inhibition of mild steel in 0.5 M sulphuric acid by some green corrosion inhibitors', J. Solid State Electrochem.,13,1743-1756. <https://doi.org/10.1007/s10008-009-0845-y>
- [56] S.S.Salem, E.N. Hammad, A.A.Mohamed, W.El-DougDoug (2022) A comprehensive review of nanomaterials: Types, synthesis, characterization, and applications. Biointerface Res Appl Chem. 13(1), 41. doi.org/ 10.33263/BRIAC131.041
- [57] I.B.Onyeachu, S.Abdel-Azeim, D.S.Chauhan, M.A.Quraishi (2020) 'Electrochemical and computational insights on the application of expired metformin drug as a novel inhibitor for the sweet corrosion of C1018 steel', ACS omega, 6(1), 65-76. doi.org/ 10.33263/BRIAC131.041
- [58] M.A.Abu-Dalo, A.A.Othman, N.A.F.Al-Rawashdeh (2012) 'Exudate gum from acacia trees as green corrosion inhibitor for mild steel in acidic media', Int. J.Electrochem. Sci., 7(10), 9303-9324. [https://doi.org/10.1016/S1452-3981\(23\)16199-2](https://doi.org/10.1016/S1452-3981(23)16199-2)
- [59] AM.A.li, A.M.Ouf, El- A.Hossiany, A.S.Fouda (2022) Eco-friendly approach to corrosion inhibition of copper in hno3 solution by the expired tylosin drug. Biointerface Res Appl Chem. 12(4),5116–30. <https://doi.org/10.33263/BRIAC124.51165130>
- [60] A.Zarrouk, B.Hammouti, A.Dafali, M.Bouachrine, H.Zarrok, S.Boukhris, S.S.Al-Deyab (2014) A theoretical study on the inhibition efficiencies of some quinoxalines as corrosion inhibitors of copper in nitric acid', J. Saudi Chem. Soc., 18(5),450-455. doi.org/10.1016/J.JSCS.2011.09.011
- [61] I.B.Obot, N.O.Obi-Egbedi (2010) 'Theoretical study of benzimidazole and its derivatives and their potential activity as corrosion inhibitors', Corros.Sci., 52(2), 657-660. <https://doi.org/10.1016/j.corsci.2009.10.017>
- [62] O.A.Elgyar, A.M.Ouf, A.El-Hossiany, A.S.Fouda (2021) The inhibition action of viscum album extract on the corrosion of carbon steel in hydrochloric acid solution. Biointerface Res Appl Chem. 11(6),14344–58. <https://doi.org/10.33263/BRIAC116.1434414358>
- [63] A.S.Fouda, E.S.El-Gharkawy, H.Ramadan, A.El-Hossiany (2021) Corrosion resistance of mild steel in hydrochloric acid solutions by clinopodium acinos as a green inhibitor. Biointerface Res Appl Chem. 11(2), 9786. doi.org/10.33263/briac112.97869803
- [64] A.S.Fouda, S.A.Abd El-Maksoud, A.A.M.Belal, A.El-Hossiany, A.Ibrahium (2018) Effectiveness of some organic compounds as corrosion inhibitors for stainless steel 201 in 1M HCl: experimental and theoretical studies. Int J Electrochem Sci. 13(10), 9826–46. <https://doi.org/10.20964/2018.10.36>

## IZVOD

### ELEKTROHEMIJSKE I TEORIJSKE PROCENE 3-(4-HLOROFENIL)-7-METIL-5H-[1, 2, 4] TRIAZOLO [3,4-B][1,3,4]TIADIAZIN-6(7H)-ONA KAO INHIBITOR KOROZIJE ZA BAKAR U OKRUŽENJU AZOTNE KISELINE

3-(4-hlorofenil)-7-metil-5H-[1,2,4]triazolo[3,4-b][1,3,4]tiadiazin-6(7H)-on (CTT) je sintetizovan i ocenjen kao inhibitor korozije za bakar u 1M HNO<sub>3</sub>. Eksperimentalnim i teorijskim metodama u kiseloj sredini određena su adsorpciona svojstva sintetizovanog CTT. Za određivanje inhibitivnog ponašanja CTT korišćene su hemijske metode kao što su metoda gubitka mase (ML), DC potenciodinamička polarizacija (PDP) i AC impedansa (EIS). Podaci dobijeni ovim metodama pokazuju da sa povećanjem koncentracije CTT-a njegova efikasnost inhibicije (%IE) raste i dostiže 91,5% pri 24k10<sup>-6</sup> M, 25°C primenom EIS tehnike. Prisustvo CTT smanjuje kapacitet dvostrukog sloja (Cdl) i poboljšava otpor prenosa naelektrisanja (Rct) u rastvoru jedne molarne azotne kiseline. CTT je inhibitor mešovito tipa iz podataka dobijenih iz krivulja polarizacije. Dobijeni podaci ukazuju da je CTT fizički adsorbovan na površinu Cu u skladu sa Langmuir adsorpcijom. Ispitivanje površinske zaštite obavljeno je pomoću skenirajuće elektronske mikroskopije (SEM), energetski disperzivnog rendgenskog zraka (EDKS) i mikroskopa atomske sile (AFM). Takođe, izračunati su i diskutovani kvantno hemijski parametri CTT-a. Rezultati nekoliko metoda se međusobno slažu.

**Ključne reči:** Inhibicija korozije, bakar, azotna kiselina, 3-(4-hlorofenil)-7-metil-5H-[1,2,4] triazolo [3,4-b][1,3,4]tiadiazin-6(7H)-on (CTT), Langmuir izoterma

Naučni rad

Rad primljen: 03.01.2024.

Rad prihvaćen: 16.01.2024.

Rad je dostupan na sajtu: [www.idk.org.rs/casopis](http://www.idk.org.rs/casopis)